# TIME WEAVER: A Conditional Time Series Generation Model

**Sai Shankar Narasimhan** [1]  **Shubhankar Agarwal** [1]  **Oguzhan Akcin** [1]  **Sujay Sanghavi** [1]  **Sandeep Chinchali** [1]

## Abstract

Imagine generating a city's electricity demand pattern based on weather, the presence of an electric vehicle, and location, which could be used for capacity planning during a winter freeze. Such real-world time series are often enriched with paired heterogeneous contextual metadata (weather, location, etc.). Current approaches to time series generation often ignore this paired metadata, and its heterogeneity poses several practical challenges in adapting existing conditional generation approaches from the image, audio, and video domains to the time series domain. To address this gap, we introduce TIME WEAVER, a novel diffusion-based model that leverages the heterogeneous metadata in the form of categorical, continuous, and even time-variant variables to significantly improve time series generation. Additionally, we show that naive extensions of standard evaluation metrics from the image to the time series domain are insufficient. These metrics do not penalize conditional generation approaches for their poor specificity in reproducing the metadata-specific features in the generated time series. Thus, we innovate a novel evaluation metric that accurately captures the specificity of conditional generation and the realism of the generated time series. We show that TIME WEAVER outperforms state-of-the-art benchmarks, such as Generative Adversarial Networks (GANs), by up to 27% in downstream classification tasks on real-world energy, medical, air quality, and traffic data sets.

## 1. Introduction

Generating synthetic time series data is useful for creating realistic variants of private data (Yoon et al., 2020), stress-testing production systems with new scenarios (Rizzato

[1] Department of ECE, University of Texas at Austin, Austin, USA. Correspondence to: Sai Shankar Narasimhan <nsaishankar@utexas.edu>.
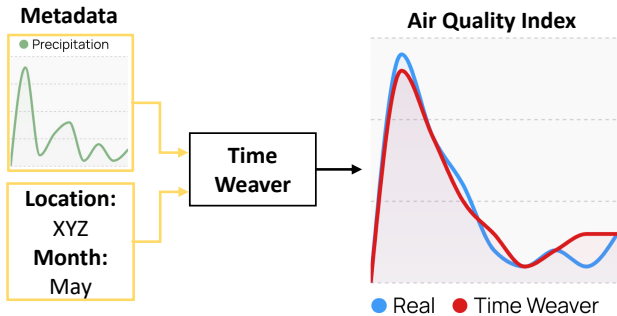
Figure 1. **TIME WEAVER generates realistic metadata-specific time series.** Consider generating the air quality index of a particular location (XYZ) given the expected precipitation (green) for a specific month (May). TIME WEAVER uses these metadata features to generate samples (red) that closely match reality (blue).

et al., 2022; Agarwal & Chinchali, 2022), asking "what-if" questions, and even augmenting imbalanced datasets (Gowal et al., 2021). Imagine generating a realistic medical electrocardiogram (ECG) pattern based on a patient's age, gender, weight, medical record, and even the presence of a pacemaker. This generated data could be used to train medical residents, sell realistic data to third parties (anonymization), or even stress-test a pacemaker's ability to detect diseases on rare variations of ECG data.

Despite potential advantages, current time series generation methods (Yoon et al., 2019; Jeha et al., 2021; Donahue et al., 2019) ignore the rich contextual metadata and, therefore, cannot be flexibly used to generate time series for specific real-world conditions. This is not due to a lack of data, as standard time series datasets have long come with paired metadata conditions. Instead, it is because today's methods are incapable of handling diverse conditions.

At first glance, generating realistic time series based on rich metadata conditions might seem like a straightforward extension of conditional image, video, or audio generation (Rombach et al., 2021; Ramesh et al., 2022; Kong et al., 2021). However, we argue that there are practical differences that make conditional time series generation and evaluation challenging, which are:

1. **Rich Metadata:** Metadata can be categorical (e.g., whether a patient has a pacemaker), quantitative (e.g., age), or even a time series, such as anticipated precipitation. Any conditional generative model for time series

should incorporate such a diverse mix of metadata conditions, as shown in Table 1. In contrast, image, video, and audio generation often deal with static text prompts.

2. **Visual Inspection of Synthetic Data Quality:** Visual inspection is a key aspect in evaluating image generation approaches as evaluation metrics like the Inception Score (IS) are widely adopted due to their alignment with human judgment. On the contrary, it is non-trivial to glance at a time series and tell if it retains key features, such as statistical moments or frequency spectra.

3. **Architectural Differences:** In the image and audio domains, we have powerful feature extractors trained on internet-scale data (Radford et al., 2021; Wu* et al., 2023). These are vital building blocks for encoding conditions in image generation (Rombach et al., 2021). However, these models are non-existent in the time series domain due to the highly irregular nature of the time series datasets with respect to horizon lengths, number of channels, and the heterogeneity of the metadata.

4. **Evaluation Metrics:** Evaluating conditional generation approaches requires a metric that captures the specificity of the generated samples with respect to its paired metadata. In Fig. 4, we show how the existing metrics, such as the time series equivalent of the standard Frechet Inception Distance (FID) score, (Jeha et al., 2021), fail to capture this specificity and only measure how close the real and generated data distributions are. This is due to the fact that these metrics completely ignore the paired metadata in their evaluation.

Given the above differences and insufficiencies in metrics, **our contributions** are:

1. We present TIME WEAVER (Fig. 1), a novel diffusion model for generating realistic multivariate time series conditioned on the paired metadata. We specifically innovate on the standard diffusion model architecture to process categorical and continuous metadata conditions.

2. We propose a new metric, the Joint Frechet Time Series Distance (J-FTSD), specifically designed to evaluate conditional time series data generation models. J-FTSD incorporates time series and metadata conditions using feature extractors trained with contrastive learning. In Sec. 6, we showcase J-FTSD's ability to accurately rank approaches based on their ability to model conditional time series data distributions.

3. We show that our approach significantly outperforms the state-of-the-art GAN models in generating high-quality, metadata-specific time series on real-world energy, healthcare, pollution, and traffic datasets (Fig. 2).

## 2. Background and Related Works

**Generative Models in Time Series:** Recently, Generative Adversarial Networks (GANs) (Donahue et al., 2019; Yoon
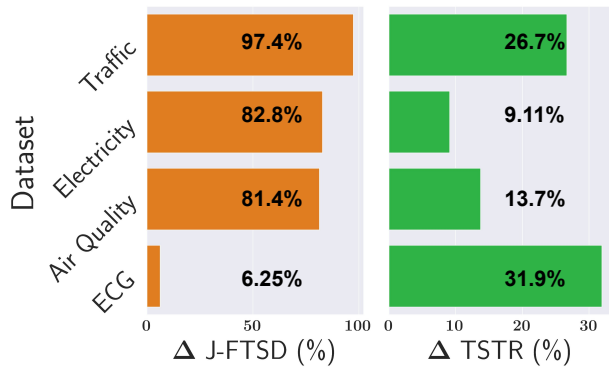


*Figure 2.* **TIME WEAVER beats GANs on all datasets for both J-FTSD and Train on Synthetic Test on Real (TSTR) metrics.** We show percentage improvement of TIME WEAVER over state-of-the-art GAN models on four diverse datasets.

et al., 2019; Li et al., 2022; Thambawita et al., 2021) have emerged as popular methods for time series data generation. However, these GAN-based approaches often struggle with unstable training and mode collapse (Chen, 2021). In response, Diffusion Models (DMs) (Sohl-Dickstein et al., 2015) have been introduced in the time series domain (Alcaraz & Strodthoff, 2023; Tashiro et al., 2021), offering more realistic data generation. DMs are a class of generative models that are shown to be state-of-the-art in a variety of domains, including image (Dhariwal & Nichol, 2021; Ho et al., 2020), speech (Chen et al., 2020; Kong et al., 2021), and video generation (Ho et al., 2022). DMs operate by defining a Markovian forward process $q$ by gradually adding noise to the clean data sample $x_0 \sim \mathcal{X}$ where $\mathcal{X}$ is the data distribution to be learned. The forward process is predetermined by fixing a noise variance schedule $\{\beta_1, \ldots, \beta_T\}$, where $\beta_t \in [0, 1]$ and $T$ is the total number of diffusion steps. The following equations describe the forward process:

$$q(x_1, \ldots, x_T \mid x_0) = \prod_{t=1}^{T} q(x_t \mid x_{t-1}), \quad (1)$$

$$q(x_t \mid x_{t-1}) = \mathcal{N}(\sqrt{1 - \beta_t} x_{t-1}, \beta_t \mathbf{I}). \quad (2)$$

During training, a clean sample $x_0$ is transformed into $x_t$ using Eq. (2). Then, a neural network, $\theta_{\text{denoiser}}(x_t, t)$, is trained to estimate the amount of noise added between $x_{t-1}$ and $x_t$ with the following loss function:

$$\mathcal{L}_{\text{DM}} = \mathbb{E}_{x \sim \mathcal{X}, \epsilon \sim \mathcal{N}(\mathbf{0}, \mathbf{I}), t \sim \mathcal{U}(1,T)} \left[ \| \epsilon - \theta_{\text{denoiser}}(x_t, t) \|_2^2 \right]. \quad (3)$$

Here, $t \sim \mathcal{U}(1, T)$ indicates that $t$ is sampled from a uniform distribution between 1 and $T$, $\epsilon$ is the noise added to $x_{t-1}$ to obtain $x_t$. In inference, we start from $x_T \sim \mathcal{N}(\mathbf{0}, \mathbf{I})$, where $\mathcal{N}(\mathbf{0}, \mathbf{I})$ represents a zero mean, unit variance Gaussian distribution, and iteratively denoise using $\theta_{\text{denoiser}}$ to obtain a clean sample from the data distribution $\mathcal{X}$, i.e., $x_T \rightarrow x_{T-1}, \ldots, x_0$. A detailed explanation of

DMs is provided in App. A.

To extend to conditional DMs, the most commonly used approach is to keep the forward process the same as in Eq. (2) and add additional conditions $c$ to the reverse process. Minimizing $||\epsilon - \theta_{\text{denoiser}}(x_t, t, c)||_2^2$ in the loss function provided in Eq. (3) facilitates learning the conditional distribution. Conditional DMs are used in image, video (Saharia et al., 2021; Lugmayr et al., 2022; Rombach et al., 2021; Ramesh et al., 2022), and speech (Kong et al., 2021) generation. These models allow for diverse conditioning inputs, such as text, image, or even segmentation maps. However, these methods rely on image-focused tools like Convolutional Neural Networks (CNNs), which struggle to maintain essential time series characteristics, including long-range dependencies, as noted in (Gu et al., 2022). For time series data, models such as CSDI (Tashiro et al., 2021) and SSSD (Alcaraz & Strodthoff, 2022) exist but are mainly limited to imputation tasks without substantial conditioning capabilities. Closest to our work, Alcaraz & Strodthoff (2023) attempts to incorporate ECG statements as metadata (only categorical) for ECG generation. However, this approach falls short as it does not consider heterogeneous metadata. Our method surpasses these limitations by effectively handling a broader range of metadata modalities, thus enabling more realistic time series data generation under varied heterogeneous conditions.

**Metrics for Conditional Time Series Generation:** Various metrics have been developed in the time series domain, focusing on the practical utility of the generated time series data. To this end, train on synthetic test on real (TSTR) metric (Jordon et al., 2018; Esteban et al., 2017) is used to assess the synthetic data's ability to capture key features of the real dataset. TSTR metrics have been widely used to evaluate unconditional time series generation. Yoon et al. (2019) proposed the predictive score where synthetic time series data is used to train a forecaster, and forecast performance is evaluated on real time series data. More traditional approaches include average cosine similarity, Jensen distance (Li et al., 2022), and autocorrelation comparisons (Lin et al., 2020; Bahrpeyma et al., 2021). However, these heuristics often fail to fully capture the nuanced performance of conditional generative models.

A more popular method to evaluate generative models is to use distance metrics between the generated and real data samples. One of the most commonly used distance metrics is the Frechet Distance (FD) (Fréchet, 1957). The FD between two multivariate Gaussian distributions $\mathcal{D}_1 \sim \mathcal{N}(\mu_1, \Sigma_1)$ and $\mathcal{D}_2 \sim \mathcal{N}(\mu_2, \Sigma_2)$ is:

$$FD(\mathcal{D}_1, \mathcal{D}_2) = ||\mu_1 - \mu_2||^2 + \text{Tr}(\Sigma_1 + \Sigma_2 - 2(\Sigma_1 \Sigma_2)^{\frac{1}{2}}). \tag{4}$$

To evaluate image generation models, the FD is adjusted to the FID (Heusel et al., 2017). FID uses a feature extractor, the Inceptionv3 model (Szegedy et al., 2015), to transform images into embeddings, upon which the FD is calculated. Similar adaptations such as Frechet Video Distance (Unterthiner et al., 2018), Frechet ChemNet Distance (Preuer et al., 2018), and Context-FID (Jeha et al., 2021) exist for other domains, employing domain-specific feature extractors. However, these metrics are designed only to evaluate unconditional data generation since they only match the true data distribution marginalizing over all the conditions.

To evaluate conditional generation models, many metrics are proposed for categorical conditions (Murray, 2019; Huang et al., 2018; Benny et al., 2020; Liu et al., 2018; Miyato & Koyama, 2018). To create a more general metric, Soloveitchik et al. (2022) proposed the conditional FID (CFID) metric that works with continuous conditionals and calculates the conditional distributions of the generated and real data given the condition. In particular, DeVries et al. (2019) propose the Frechet Joint Distance (FJD), where the embeddings of the image and condition are obtained with different embedding functions and concatenated to create a joint embedding space. DeVries et al. (2019) consider conditions that are classes (image category), text descriptions (image captions), or images (for tasks like style transfer). However, in our case, the metadata could be any arbitrary combination of categorical, continuous conditions that might vary over time. Additionally, like other metrics considered in the literature, FJD is defined for image generation and does not consider the unique characteristics of time series data. In contrast, our proposed metric, J-FTSD, is specifically designed for evaluating time series data generation models conditioned on heterogeneous metadata.

## 3. Problem Formulation

Consider a multivariate time series sample $x \in \mathbb{R}^{L \times F}$, where $L$ denotes the time series horizon and $F$ denotes the number of channels. Each sample $x$ is associated with metadata $c$, comprising categorical features $c_{\text{cat}} \in \mathbb{N}^{L \times K_{\text{cat}}}$ and continuous features $c_{\text{cont}} \in \mathbb{R}^{L \times K_{\text{cont}}}$. Here, $K_{\text{cat}}$ and $K_{\text{cont}}$ indicate the total numbers of categorical and continuous metadata features, respectively. These features are concatenated as $c = c_{\text{cat}} \oplus c_{\text{cont}}$, where $\oplus$ represents the vector concatenation operation. Thus, the metadata domain is defined as $\mathbb{N}^{L \times K_{\text{cat}}} \times \mathbb{R}^{L \times K_{\text{cont}}}$. Note that the domains of $c_{\text{cat}}$ and $c_{\text{cont}}$ allow time-varying metadata features.

*Example:* Consider generating time series data representing traffic volume on a highway ($F = 1$) over a 96-hour period ($L = 96$), using paired metadata. This metadata includes seven time-varying categorical features such as holidays (12 unique labels) and weather descriptions (11 unique labels), denoted by $K_{\text{cat}} = 7$. It also includes four time-varying continuous features like expected temperature and rain forecast, represented by $K_{\text{cont}} = 4$.
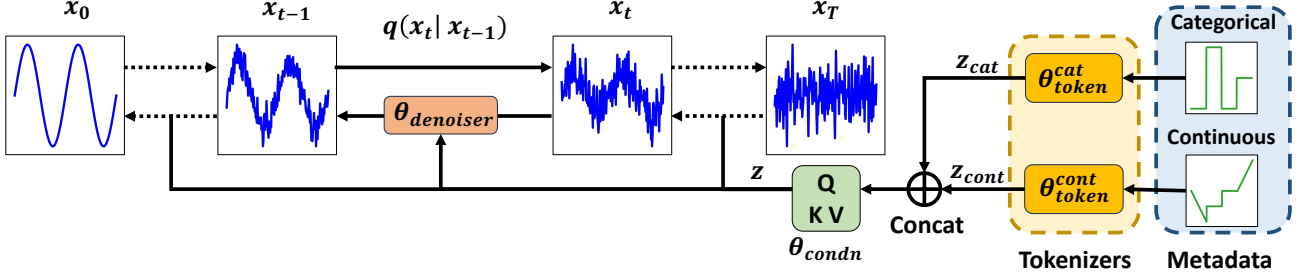
*Figure 3.* **TIME WEAVER architecture for incorporating metadata in the diffusion process:** This figure shows the training process of TIME WEAVER model. Starting from the original sample $x_0$ (on the left), we gradually add noise through a forward process $q(x_t \mid x_{t-1})$ resulting in noisy samples $x_t$. In the reverse process, first, the categorical and continuous metadata are preprocessed with tokenizers $\theta_{\text{token}}^{\text{cat}}$ and $\theta_{\text{token}}^{\text{cont}}$ respectively. Then, we concatenate their output and process it through a self-attention layer $\theta_{\text{condn}}$ to create the metadata embedding $z$. This embedding, along with the noisy sample $x_t$, is fed into the denoiser model $\theta_{\text{denoiser}}$. All the models are trained jointly to iteratively reconstruct a less noisy sample $x_{t-1}$. This denoising process is repeated until the original sample $x_0$ is reconstructed.

We denote the dataset $D_{x,c} = \{(x_i, c_i)\}_{i=1}^n$ consisting of $n$ independent and identically distributed (i.i.d) samples of time series data $x$ and paired metadata $c$, sampled from a joint distribution $p(x, c)$. **Our objective is to** develop a conditional generation model $G$, such that the samples generated by $G(c)$, distributionally match $p(x|c)$.

## 4. Conditional Time Series Generation using TIME WEAVER

Our approach, TIME WEAVER, is a diffusion-based conditional generation model. We choose DMs over GANs as we consider heterogenous metadata, i.e., the metadata can contain categorical, continuous, or even time-varying features. Previous works show that the conditional variants of GANs suffer from mode collapse when dealing with continuous conditions (Ding et al., 2020). Additionally, the proposed alternatives have not been tested in the time series domain for heterogeneous metadata. Our TIME WEAVER model consists of two parts - a denoiser backbone that generates data and a preprocessing module that processes the time-varying categorical and continuous metadata variables.

**Metadata Preprocessing:** The preprocessing step involves handling the metadata $c = c_{\text{cat}} \oplus c_{\text{cont}}$. Here, $c_{\text{cat}} \in \mathbb{N}^{L \times K_{\text{cat}}}$ and $c_{\text{cont}} \in \mathbb{R}^{L \times K_{\text{cont}}}$ represent time-varying categorical and continuous metadata features respectively (see Sec. 3). To better incorporate these features from different modalities, we process them separately and then combine them with a self-attention layer.

- The categorical tokenizer $\theta_{\text{token}}^{\text{cat}}$ first converts each category in $c_{\text{cat}}$ into one-hot encoding and then processes with fully connected (FC) layers to create categorical embedding $z_{\text{cat}} \in \mathbb{R}^{L \times d_{\text{cat}}}$. Similarly, the continuous tokenizer $\theta_{\text{token}}^{\text{cont}}$ also uses FC layers to encode continuous metadata $c_{\text{cont}}$ into continuous embeddings $z_{\text{cont}} \in \mathbb{R}^{L \times d_{\text{cont}}}$. Using FC layers allows the model to learn the inherent correlation between the different metadata fea-

tures within the categorical and continuous domains. Using FC layers is just a design choice, and more sophisticated layers can also be used.

- $z_{\text{cat}}$ and $z_{\text{cont}}$ are then concatenated and passed into a self-attention layer $\theta_{\text{condn}}$ to generate the metadata embedding $z \in \mathbb{R}^{L \times d_{\text{meta}}}$. The self-attention layer equips the generative model to capture the temporal relationship between the different metadata features.

Here, $d_{\text{cat}}$, $d_{\text{cont}}$, and $d_{\text{meta}}$ are design choices, and we refer the reader to App. D for further details.

**Denoiser:** As the denoiser backbone for TIME WEAVER, we rely on two state-of-the-art architectures - CSDI (Tashiro et al., 2021) and SSSD (Alcaraz & Strodthoff, 2022). The CSDI model uses feature and temporal self-attention layers to process sequential time series data, while SSSD uses structured state-space layers. Note that these denoiser models are designed for imputation and forecasting tasks, so they are designed to take unimputed and historical time series as respective inputs. We modify these denoisers into more flexible metadata-conditioned time series generators by augmenting them with preprocessing layers ($\theta_{\text{token}}^{\text{cat}}$, $\theta_{\text{token}}^{\text{cont}}$, and $\theta_{\text{condn}}$). We refer the reader to App. D for details regarding architectural changes. We train the preprocessing layers $\theta_{\text{condn}}$, $\theta_{\text{token}}^{\text{cont}}$, and $\theta_{\text{token}}^{\text{cat}}$, and the denoiser $\theta_{\text{denoiser}}$ jointly with the following loss:

$$\mathcal{L}_{(\theta_{\text{denoiser}}, \theta_{\text{condn}}, \theta_{\text{token}}^{\text{cont}}, \theta_{\text{token}}^{\text{cat}})} = \mathbb{E}_{x, c \sim D_{x,c}, \epsilon \sim \mathcal{N}(\mathbf{0}, \mathbf{I}), t \sim \mathcal{U}(1, T)}$$
$$[\|\epsilon - \theta_{\text{denoiser}}(x_t, t, z)\|_2^2], \quad (5)$$

where $z = \theta_{\text{condn}}(\theta_{\text{token}}^{\text{cat}}(c_{\text{cat}}) \oplus \theta_{\text{token}}^{\text{cont}}(c_{\text{cont}}))$, $D_{x,c}$ represents the dataset of time series and paired metadata sampled from the joint distribution $p(x, c)$, and $T$ is the total number of diffusion steps. As explained in Sec. 2, minimizing the loss in Eq. (5), allows TIME WEAVER to learn how to generate samples from the conditional distribution $p(x|c)$. During inference, we start from $x_T \sim \mathcal{N}(\mathbf{0}, \mathbf{I})$ and iteratively denoise (with metadata $c$ as input) for $T$ steps to generate $x_0 \sim p(x|c)$. This process is depicted in Fig. 3.

4

# 5. Joint Frechet Time Series Distance

A good distance metric should penalize the conditional generation approach (provide higher values) if the real and generated joint distributions of the time series and the paired metadata do not match. Existing metrics such as Context-FID (Jeha et al., 2021) rely only on the time series feature extractor, and the metric computation does not involve the paired metadata. This prevents these metrics from penalizing conditional generation approaches for their inability to reproduce metadata-specific features in the generated time series. Therefore, we propose a new metric to evaluate metadata-conditioned time series generation, the Joint Frechet Time Series Distance (J-FTSD).

In J-FTSD, we compute the FD between the real and generated joint distributions of time series and the paired metadata. Consider samples from a real data distribution indicated by $D_r = \{(x_1^r, c_1), \ldots, (x_n^r, c_n)\}$, where $x_i^r$ indicates the time series and $c_i$ indicates the paired metadata. We denote the dataset of generated time series and the corresponding metadata as $D_g = \{(x_1^g, c_1), \ldots, (x_n^g, c_n)\}$, where $x_i^g = G(c_i) \, \forall i \in [1, n]$, and $G$ denotes any arbitrary conditional generation model defined in Sec. 3. First, similar to the FID and FJD computations, we project the time series and the paired metadata into a lower-dimensional embedding space using $\phi_{\text{time}}(\cdot) : \mathbb{R}^{L \times F} \to \mathbb{R}^{d_{\text{emb}}}$ and $\phi_{\text{meta}}(\cdot) : \mathbb{R}^{L \times K} \to \mathbb{R}^{d_{\text{emb}}}$ as respective feature extractors, where $d_{\text{emb}}$ is the size of the embedding. We concatenate these time series and metadata embeddings to create a joint embedding space. We then calculate the FD over the joint embedding space. As such J-FTSD is formally defined as:

$$
\begin{aligned}
\text{J-FTSD}(D_g, D_r) = \, & \|\mu_{z^r} - \mu_{z^g}\|^2 \\
& + \text{Tr}(\Sigma_{z^r} + \Sigma_{z^g} - 2(\Sigma_{z^r}\Sigma_{z^g})^{\frac{1}{2}}).
\end{aligned} \tag{6}
$$

Here, $\mu_{z^d}$ and $\Sigma_{z^d}$ for $d \in \{g, r\}$ are calculated as:

$$
z_i^d = \phi_{\text{time}}(x_i^d) \oplus \phi_{\text{meta}}(c_i) \qquad \forall i : (x_i^d, c_i) \in D_d,
$$

$$
\mu_{z^d} = \frac{1}{n}\sum_{i=1}^{n} z_i^d, \; \Sigma_{z^d} = \frac{1}{n-1}\sum_{i=1}^{n}(z_i^d - \mu_{z^d})(z_i^d - \mu_{z^d})^\top.
$$

In essence, J-FTSD computes the FD between the Gaussian approximations of the real and generated joint embedding datasets. In Eq. (6), $\mu_{z^r}$, $\mu_{z^g}$ and $\Sigma_{z^r}$, $\Sigma_{z^g}$ are the mean and the variance of the Gaussian approximation of the real and generated joint embedding dataset respectively.

**Training Feature Extractors:** Now, we describe our approach to obtain the feature extractors $\phi_{\text{time}}$ and $\phi_{\text{meta}}$. As explained in Sec. 2, DeVries et al. (2019) suggest using separate encoders for data samples and conditions. However, they only deal with a specific type of condition, and this naturally poses a problem for a straightforward extension of their approach to our case, where the metadata could be any arbitrary combination of categorical, continuous, and time-varying features. As such, we propose a novel approach to train the feature extractors $\phi_{\text{meta}}$ and $\phi_{\text{time}}$ specific to the time series domain. We jointly train $\phi_{\text{time}}$ and $\phi_{\text{meta}}$ with contrastive learning to better capture the joint distribution of the time series and paired metadata, as contrastive learning is a commonly used method to map data coming from various modalities into a shared latent space (Yuan et al., 2021; Zhang et al., 2022; Ramesh et al., 2022).

---

**Algorithm 1** One iteration for training time series $\phi_{\text{time}}$ and metadata $\phi_{\text{meta}}$ feature extractors.

---

**input** Time series feature extractor $\phi_{\text{time}}$, Metadata feature extractor $\phi_{\text{meta}}$, Time series batch $X_{\text{batch}}$, Paired Metadata batch $C_{\text{batch}}$, Number of patches $N_{\text{patch}}$, Patch length $L_{\text{patch}}$, Batch size $N_{\text{batch}}$.

1: Randomly select $N_{\text{patch}}$ patches of length $L_{\text{patch}}$ from each sample in $X_{\text{batch}}$ and $C_{\text{batch}}$ to generate $X_{\text{batch}}^{\text{patch}}$ and $C_{\text{batch}}^{\text{patch}}$.
2: Obtain the time series and metadata embedding - $\phi_{\text{time}}(X_{\text{batch}}^{\text{patch}})$ and $\phi_{\text{meta}}(C_{\text{batch}}^{\text{patch}})$ respectively.
3: Obtain the `logits` - $\phi_{\text{time}}(X_{\text{batch}}^{\text{patch}})^T \phi_{\text{meta}}(C_{\text{batch}}^{\text{patch}})$.
4: Define the `labels` - $[0, 1, 2, \ldots, N_{\text{batch}} \times N_{\text{patch}} - 1]$.
5: Compute $\mathcal{L}_{\text{time}} = \mathcal{L}_{\text{CE}}(\texttt{logits}, \texttt{labels})$.
6: Compute $\mathcal{L}_{\text{meta}} = \mathcal{L}_{\text{CE}}(\texttt{logits.T}, \texttt{labels})$.
7: Compute $\mathcal{L}_{\text{total}} = (\mathcal{L}_{\text{time}} + \mathcal{L}_{\text{meta}})/2$.
8: Update parameters of $\phi_{\text{time}}$ and $\phi_{\text{meta}}$ to minimize $\mathcal{L}_{\text{total}}$.

---

Algorithm 1 summarizes one training iteration of our feature extractors $\phi_{\text{time}}$ and $\phi_{\text{meta}}$ as also visually depicted in App. C. Given the batch of time series $X_{\text{batch}}$ and metadata $C_{\text{batch}}$, we randomly pick $N_{\text{patch}}$ patches with horizon $L_{\text{patch}}$ from each time series and metadata sample in batches $X_{\text{batch}}$ and $C_{\text{batch}}$ (line 1). Then, we obtain the time series and metadata embeddings for all patches through their respective feature extractors, $\phi_{\text{time}}$ for time series and $\phi_{\text{meta}}$ for metadata (line 2). Finally, we compute the dot product of time series and metadata embeddings (line 3), and obtain the symmetric cross-entropy loss (line 5 - 7), which is used to jointly update parameters of $\phi_{\text{time}}$ and $\phi_{\text{meta}}$ (line 8).

In essence, we learn a joint embedding space for time series and metadata by jointly training $\phi_{\text{time}}$ and $\phi_{\text{meta}}$. This is achieved by adjusting the feature extractors' parameters to maximize the cosine similarity of the time series embeddings and the metadata embeddings of $N_{\text{batch}} \times N_{\text{patch}}$ pairs of time series and paired metadata in the batch. In our experiments, we used the Informer encoder architecture (Zhou et al., 2021) for $\phi_{\text{time}}$ and $\phi_{\text{meta}}$. We choose $L_{\text{patch}}$ based on the length of the smallest chunk of the time series that contains metadata-specific features. We refer the readers to App. C for further details on the choices of $N_{\text{patch}}$, $L_{\text{patch}}$, and the encoder architecture.

| DATASET | HORIZON | # CHANNELS | CATEGORICAL FEATURES | CONTINUOUS FEATURES |
|---------|---------|-----------|---------------------|---------------------|
| AIR QUALITY (CHEN, 2019) | 96 | 6 | 12 STATIONS, 5 YEARS, 12 MONTHS, 31 DATES, 24 HOURS, 17 WIND DIRECTIONS | TEMPERATURE, PRESSURE, DEW POINT TEMPERATURE, RAIN LEVELS, WIND SPEED |
| TRAFFIC (HOGUE, 2019) | 96 | 1 | 12 HOLIDAYS, 7 YEARS, 12 MONTHS, 31 DATES, 24 HOURS, 11 BROAD WEATHER DESCRIPTIONS, 38 FINE WEATHER DESCRIPTIONS | TEMPERATURE, RAIN LEVELS, SNOW FALL LEVELS, CLOUD CONDITIONS |
| ELECTRICITY (TRINDADE, 2015) | 96 | 1 | 370 USERS, 4 YEARS, 12 MONTHS, 31 DATES | N.A. |
| ECG (WAGNER ET AL., 2020) | 1000 | 8 | 71 HEART DISEASE STATEMENTS | N.A. |

*Table 1.* **Dataset overview for experiments with TIME WEAVER.** This table outlines the key characteristics of the datasets employed in our experiments. These datasets, encompassing Air Quality, Traffic, Electricity, and ECG, have been selected to demonstrate TIME WEAVER's versatility across different time horizons (*col 1*), number of channels (*col 2*), and a wide range of metadata types (*col 3,4*).
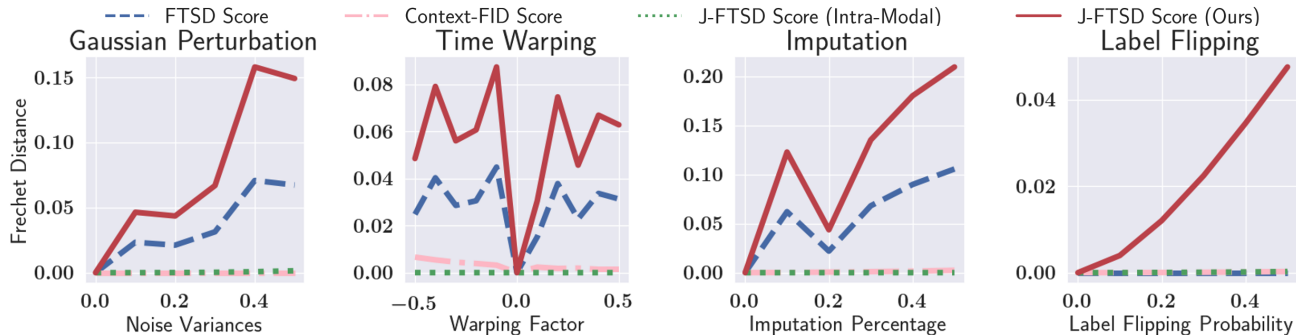


*Figure 4.* **J-FTSD metric correctly penalizes the conditional time series data distribution.** A good metric should penalize the conditional generation approaches for not being specific to the metadata and deviating from real time series data distribution. As such, we compare the sensitivity of different distance metrics under various synthetic disturbances on the Air Quality dataset (starting from the left); we add Gaussian noise, warp, impute, and randomly change the metadata of the time series samples. We clearly show that as the amount of perturbation increases, our J-FTSD metric (in red) shows the highest sensitivity, correctly capturing the dissimilarities between the perturbed and the original datasets, while the other metrics remain unchanged or show lower sensitivity.

**Why is J-FTSD a good metric to evaluate conditional generation models?** One aspect of the J-FTSD computation involves estimating the covariance between the time series and the metadata embeddings. Additionally, jointly training the feature extractors with contrastive learning aids in effectively capturing the correlation between the time series and the metadata embeddings. Therefore, the covariance term decreases if the generated time series does not contain metadata-specific features. This allows J-FTSD to accurately penalize for the differences between the real and generated joint distributions, which directly translates to penalizing conditional generation approaches for their poor specificity in reproducing metadata-specific features.

## 6. Experiments

We evaluated the performance of TIME WEAVER across datasets featuring a diverse mix of seasonalities, discrete and continuous metadata conditions, a wide range of horizons, and multivariate correlated channels. The list of datasets and their metadata features are provided in Table 1. All models are trained on the train split, while all metrics are reported on the test split, further detailed in App. B.

**Baselines:** We represent the results for the CSDI and SSSD backbones for TIME WEAVER as TIME WEAVER-CSDI

and TIME WEAVER-SSSD, respectively. Since there are no existing approaches for metadata-conditioned time series generation with categorical, continuous, and time-variant metadata features, we modify the existing state-of-the-art GAN approaches to incorporate metadata conditions, similar to TIME WEAVER. The GAN baselines include CNN based approaches like WaveGAN (Donahue et al., 2019), an audio-focused GAN model, and Pulse2Pulse (Thambawita et al., 2021), a model specializing in Deep-Fake generation. The exact training details are provided in App. D and E. We additionally tried comparing with TimeGAN (Yoon et al., 2019), a Recurrent Neural Network (RNN) based approach, and TTS-GAN (Li et al., 2022), a Transformer-based approach. However, both of these GAN models did not converge on any of the datasets. We show their training results in App. E.2.

**Evaluation Metrics:** We evaluate our approaches and the GAN baselines using the J-FTSD metric, as detailed in Sec. 5. To validate the correctness of J-FTSD's evaluation, we also report the area under the curve (AUC) scores of a classifier trained only using synthetic data. The classifier is trained to predict the metadata given the corresponding synthetic time series. We then test this classifier on the real unseen test dataset. High accuracy indicates that our synthetic data faithfully retained critical features of the paired

6

| APPROACH | AIR QUALITY | | ECG | | TRAFFIC | | ELECTRICITY | |
|---|---|---|---|---|---|---|---|---|
| | J-FTSD ↓ | TSTR ↑ | J-FTSD ↓ | TSTR ↑ | J-FTSD ↓ | TSTR ↑ | J-FTSD ↓ | TSTR ↑ |
| WAVEGAN (DONAHUE ET AL., 2019) | 11.7350 | 0.6523 | 9.4243 | 0.6115 | 23.0099 | 0.5675 | 7.8620 | 0.5757 |
| PULSE2PULSE (THAMBAWITA ET AL., 2021) | 20.9333 | 0.5874 | 12.8096 | 0.6002 | 16.6357 | 0.5409 | 3.1805 | 0.6895 |
| TIME WEAVER-CSDI | **2.1869** | **0.7419** | **8.8352** | **0.8067** | 0.8359 | **0.7189** | **0.5465** | **0.7523** |
| TIME WEAVER-SSSD | 10.1885 | 0.6826 | 19.0671 | 0.49 | **0.4347** | 0.6562 | 1.0505 | 0.7456 |

*Table 2.* **DM-based approaches outperform GAN-based approaches on J-FTSD and TSTR metrics**. The table shows the performance of all the models (rows) on specified datasets (columns). TIME WEAVER-CSDI variant significantly outperforms GANs in both metrics. TIME WEAVER-SSSD only underperforms for the ECG dataset, but still outperforms GANs on all other datasets. Our experimental findings also confirm that lower J-FTSD scores correspond to higher AUC (TSTR) scores when tested on the original test dataset, showcasing the utility of our proposed J-FTSD metric in evaluating the quality of the generated data distribution.

metadata. For the classifier, we use a standard ResNet-1D (He et al., 2016) model. We denote this metric as TSTR in Table 2. For each dataset, the categories for which we train the classifier are: Electricity - Months (12), Air Quality - Station (12), Traffic - Weather Description (11), and ECG - Heart Conditions - (71). The exact training steps of the classifiers are outlined in App. F.

**Experimental Results and Analysis:** Our experiments demonstrate that the TIME WEAVER models significantly outperform baseline models in synthesizing time series data across all evaluated benchmarks. Our experiments address the following key questions:

**Does the J-FTSD metric correctly penalize when the generated time series samples are not specific to the paired metadata?** In Fig. 4, we assess the sensitivity of our J-FTSD metric against previous Frechet distance-based metrics. This assessment involves introducing controlled perturbations into the time series to test the sensitivity of the metric. These perturbations include *Gaussian noise-*which introduces Gaussian noise of increasing variance; *time warping*, involving scaling adjustments; *imputation-*imputing the time series with local mean and *label flipping-*where metadata conditions are randomly changed, decoupling them from the time series. An effective metric should demonstrate an increased sensitivity when the real and generated joint distributions of time series and metadata diverge. We compare against three Frechet distance-based metrics: 1) FTSD score, which calculates the Frechet distance using only time series embeddings (derived from the $\phi_{time}$ feature extractor). 2) The Context-FID score (Jeha et al., 2021), where the $\phi_{time}$ feature extractor is trained to maximize similarity for similar time series. 3) The J-FTSD (Intra-Modal) score, which is calculated the same way as J-FTSD, but the time series and metadata feature extractors are trained individually to maximize the embedding similarity for similar samples. Our J-FTSD metric is the most sensitive compared to other metrics under synthetic disturbances. The key benefit of our metric can be observed in the label-flipping experiment, where only our metric increases as we increase the label-flipping probability in the paired metadata conditions. Other metrics remain un-

changed and lack sufficient sensitivity because other metrics overlook paired metadata in their distance calculations, a critical factor that J-FTSD adeptly incorporates. Additionally, the J-FTSD (Intra-Modal) score remains mostly unchanged under these perturbations, showing the advantage of jointly training time series and metadata feature extractors as we do in our metric. Experiments in Fig. 4 underscore the importance of our J-FTSD metric in assessing the quality and specificity of the generated time series data.

**Does the distribution of synthetic data generated by TIME WEAVER match the real data distribution?** Across all the datasets, TIME WEAVER-CSDI variant consistently outperform GAN models in terms of J-FTSD scores, as shown in Table 2. Specifically, for the J-FTSD score, we beat the best GAN model by roughly $5\times$ on the Air Quality dataset, $1.05\times$ on the ECG dataset, $38\times$ on the Traffic dataset, and $5\times$ on the Electricity dataset.

**Does the synthetic data generated by TIME WEAVER capture metadata-specific features to train an accurate classifier?** When training with the generated synthetic time series data, the classifier's accuracy in classifying metadata hinges on the presence of distinct metadata-specific features in the time series. The high TSTR scores in Table 2 strongly suggest that the data generated by TIME WEAVER retain the essential characteristics necessary to train classifiers that exhibit high AUC on real unseen test data. The marked improvement in TSTR scores with TIME WEAVER, compared to GAN models, demonstrates both the practical value and the superior quality of the synthetic data generated by our model. The TIME WEAVER-SSSD model fails to learn metadata-specific features only for the ECG dataset, showing subpar results for both metrics.

**Does the lower J-FTSD correlate with higher TSTR performance?** The experimental data, as outlined in Table 2, exhibit a clear correlation: lower J-FTSD scores are consistently associated with higher TSTR scores on the original, unseen test dataset. This correlation is anticipated, given that both metrics evaluate the precision of the time series relative to the corresponding metadata and the closeness of the real and synthetic joint distributions. This fur-
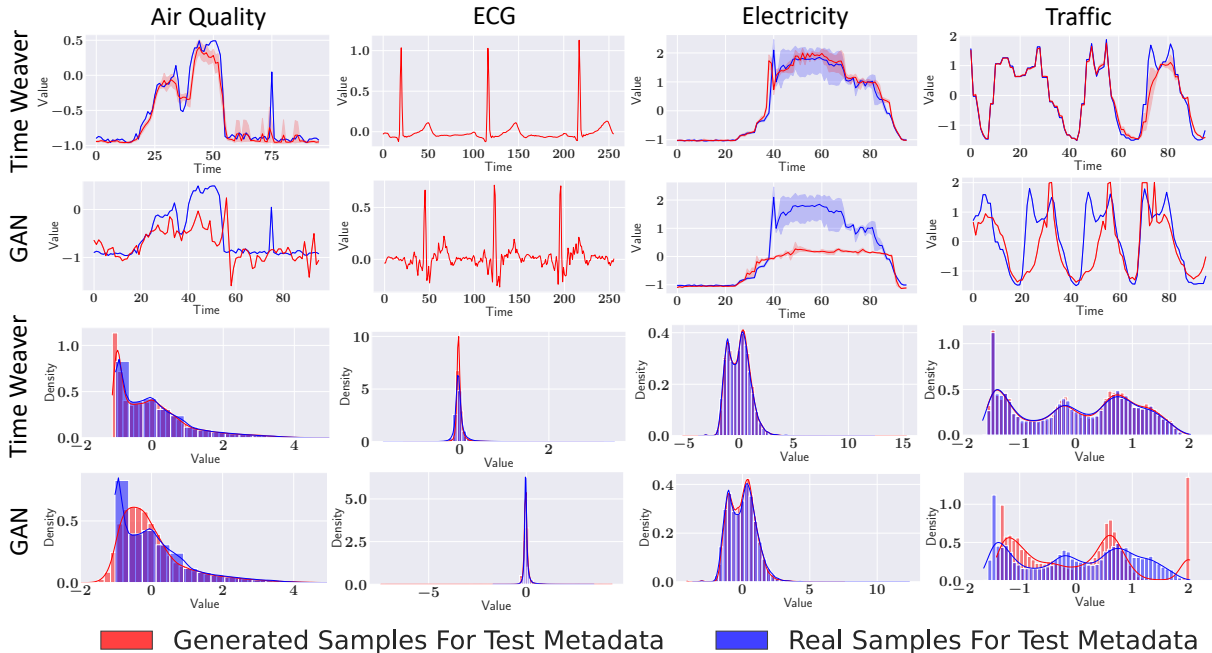
*Figure 5.* **TIME WEAVER generated time series distribution matches with the real time series distribution.** Each column represents a different dataset. The real time series is in blue, while the generated time series is in red. The first & third rows correspond to the TIME WEAVER model, and the second & fourth rows correspond to the best-performing GAN model. The top two rows have the time series for an unseen test metadata condition, and the bottom two rows have the comparison between the frequency distributions of the real and generated time series datasets also for the unseen test metadata condition. Both results indicate that our TIME WEAVER model can generate realistic time series samples that are specific to the corresponding metadata condition, beating the previous state-of-the-art GAN model. In both scenarios, the GAN models fail to match the real time series and data distribution, while our TIME WEAVER model has learned the correct conditional distribution for the specific metadata condition, specifically for the Air Quality and Traffic datasets.

ther underscores the effectiveness of the J-FTSD metric as a reliable indicator to assess the quality of generated data.

**Does the synthetic data generated by TIME WEAVER qualitatively match the real data?** Figure 5 (top two rows) displays the quality and realism of the time series data generated by the best performing TIME WEAVER model. This figure contrasts generated time series samples with real ones under identical metadata conditions. The comparison demonstrates that the TIME WEAVER model produces time series samples highly similar to real samples, effectively mapping metadata to the corresponding time series. In contrast, GAN baseline models face challenges in generating realistic time series and accurately mapping metadata. A notable example is their performance with ECG signals (2nd column): GAN models only learn to generate a noisy version of the ECG samples while our TIME WEAVER model generates a pristine realistic sample. We provide additional qualitative samples in App. G.

**Does the synthetic data generated by TIME WEAVER and the real data match in terms of density and spread of time series values?** In Fig. 5 (bottom two rows), we extend our analysis to compare real and generated data distributions across all datasets. This is achieved by transforming real and generated time series datasets into fre-

quency distributions over their respective values. Take, for instance, the traffic dataset: we aggregate all time series from the dataset to form a frequency distribution over their raw values for both real and generated datasets. The TIME WEAVER model demonstrates a significantly more accurate representation of the real time series distribution than the best performing GAN. GAN models consistently fail to learn the complex underlying distributions of real data, particularly evident in the Air Quality and Traffic datasets.

## 7. Conclusion

This paper addresses a critical gap in synthetic time series data generation by introducing TIME WEAVER, a novel diffusion-based generative model. TIME WEAVER leverages heterogeneous paired metadata, encompassing categorical, continuous, and time-variant variables, to significantly improve the quality of generated time series. Moreover, we introduce a new evaluation metric, J-FTSD, to assess conditional time series generation models. This metric offers a refined approach to evaluating the specificity of generated time series relative to paired metadata conditions. Through TIME WEAVER , we demonstrate state-of-the-art results across four diverse real-world datasets.

**Limitations:** Despite its superior performance in gener-

ating realistic time series data, TIME WEAVER encounters challenges typical of DMs, including slower inference and prolonged training durations compared to GAN-based models. Future work will focus on overcoming these limitations, potentially through techniques such as progressive distillation (Salimans & Ho, 2022) for accelerated inference. We also aim to explore the application of heterogeneous paired metadata conditions to enhance forecasting and anomaly detection within the time series domain.

# References

Agarwal, S. and Chinchali, S. P. Synthesizing adversarial visual scenarios for model-based robotic control. In *6th Annual Conference on Robot Learning*, 2022.

Alcaraz, J. L. and Strodthoff, N. Diffusion-based time series imputation and forecasting with structured state space models. *Transactions on Machine Learning Research*, 2022. ISSN 2835-8856. URL https://openreview.net/forum?id=hHiIbk7ApW.

Alcaraz, J. M. L. and Strodthoff, N. Diffusion-based conditional ecg generation with structured state space models. *Computers in Biology and Medicine*, pp. 107115, 2023.

Bahrpeyma, F., Roantree, M., Cappellari, P., Scriney, M., and McCarren, A. A methodology for validating diversity in synthetic time series generation. *MethodsX*, 8:101459, 2021. ISSN 2215-0161. doi: https://doi.org/10.1016/j.mex.2021.101459. URL https://www.sciencedirect.com/science/article/pii/S2215016121002521.

Benny, Y., Galanti, T., Benaim, S., and Wolf, L. Evaluation metrics for conditional image generation. *International Journal of Computer Vision*, 129:1712 – 1731, 2020. URL https://api.semanticscholar.org/CorpusID:216553817.

Chen, H. Challenges and corresponding solutions of generative adversarial networks (gans): A survey study. *Journal of Physics: Conference Series*, 1827(1): 012066, mar 2021. doi: 10.1088/1742-6596/1827/1/012066. URL https://dx.doi.org/10.1088/1742-6596/1827/1/012066.

Chen, N., Zhang, Y., Zen, H., Weiss, R. J., Norouzi, M., and Chan, W. Wavegrad: Estimating gradients for waveform generation. In *International Conference on Learning Representations*, 2020.

Chen, S. Beijing Multi-Site Air-Quality Data. UCI Machine Learning Repository, 2019. DOI: https://doi.org/10.24432/C5RK5G.

DeVries, T., Romero, A., Pineda, L., Taylor, G. W., and Drozdzal, M. On the evaluation of conditional GANs. *arXiv preprint arXiv:1907.08175*, 2019.

Dhariwal, P. and Nichol, A. Diffusion models beat gans on image synthesis. *Advances in neural information processing systems*, 34:8780–8794, 2021.

Ding, X., Wang, Y., Xu, Z., Welch, W. J., and Wang, Z. J. Ccgan: Continuous conditional generative adversarial networks for image generation. In *International conference on learning representations*, 2020.

Donahue, C., McAuley, J., and Puckette, M. Adversarial audio synthesis. In *ICLR*, 2019.

Du, W., Côté, D., and Liu, Y. Saits: Self-attention-based imputation for time series. *Expert Systems with Applications*, 219:119619, June 2023. ISSN 0957-4174. doi: 10.1016/j.eswa.2023.119619. URL http://dx.doi.org/10.1016/j.eswa.2023.119619.

Esteban, C., Hyland, S. L., and Rätsch, G. Real-valued (medical) time series generation with recurrent conditional gans, 2017.

Fréchet, M. Sur la distance de deux lois de probabilité. *Annales de l'ISUP*, VI(3):183–198, 1957. URL https://hal.science/hal-04093677.

Gowal, S., Rebuffi, S., Wiles, O., Stimberg, F., Calian, D. A., and Mann, T. A. Improving robustness using generated data. In Ranzato, M., Beygelzimer, A., Dauphin, Y. N., Liang, P., and Vaughan, J. W. (eds.), *Advances in Neural Information Processing Systems 34: Annual Conference on Neural Information Processing Systems 2021, NeurIPS 2021, December 6-14, 2021, virtual*, pp. 4218–4233, 2021. URL https://proceedings.neurips.cc/paper/2021/hash/21ca6d0cf2f25c4dbb35d8dc0b679c3f-Abstract.html.

Gu, A., Goel, K., and Re, C. Efficiently modeling long sequences with structured state spaces. In *International Conference on Learning Representations*, 2022. URL https://openreview.net/forum?id=uYLFoz1vlAC.

He, K., Zhang, X., Ren, S., and Sun, J. Identity mappings in deep residual networks. In *Computer Vision–ECCV 2016: 14th European Conference, Amsterdam, The Netherlands, October 11–14, 2016, Proceedings, Part IV 14*, pp. 630–645. Springer, 2016.

Heusel, M., Ramsauer, H., Unterthiner, T., Nessler, B., and Hochreiter, S. Gans trained by a two time-scale update rule converge to a local nash equilibrium. In *Proceedings*

*of the 31st International Conference on Neural Information Processing Systems*, NIPS'17, pp. 6629–6640, Red Hook, NY, USA, 2017. Curran Associates Inc. ISBN 9781510860964.

Ho, J., Jain, A., and Abbeel, P. Denoising diffusion probabilistic models. *Advances in neural information processing systems*, 33:6840–6851, 2020.

Ho, J., Salimans, T., Gritsenko, A., Chan, W., Norouzi, M., and Fleet, D. J. Video diffusion models. *arXiv:2204.03458*, 2022.

Hogue, J. Metro Interstate Traffic Volume. UCI Machine Learning Repository, 2019. DOI: https://doi.org/10.24432/C5X60B.

Huang, X., Liu, M.-Y., Belongie, S., and Kautz, J. Multimodal unsupervised image-to-image translation. In *Proceedings of the European Conference on Computer Vision (ECCV)*, pp. 172–189, 2018.

Jeha, P., Bohlke-Schneider, M., Mercado, P., Kapoor, S., Nirwan, R. S., Flunkert, V., Gasthaus, J., and Januschowski, T. Psa-gan: Progressive self attention gans for synthetic time series. In *International Conference on Learning Representations*, 2021.

Jordon, J., Yoon, J., and van der Schaar, M. Pategan: Generating synthetic data with differential privacy guarantees. In *International Conference on Learning Representations*, 2018. URL https://api.semanticscholar.org/CorpusID:53342261.

Kong, Z., Ping, W., Huang, J., Zhao, K., and Catanzaro, B. Diffwave: A versatile diffusion model for audio synthesis. In *9th International Conference on Learning Representations, ICLR 2021*, 2021.

Li, X., Metsis, V., Wang, H., and Ngu, A. H. H. Tts-gan: A transformer-based time-series generative adversarial network. In *Conference on Artificial Intelligence in Medicine in Europe*, 2022. URL https://api.semanticscholar.org/CorpusID:246634793.

Lin, Z., Jain, A., Wang, C., Fanti, G., and Sekar, V. Using gans for sharing networked time series data: Challenges, initial promise, and open questions. In *Proceedings of the ACM Internet Measurement Conference*, IMC '20, pp. 464–483, New York, NY, USA, 2020. Association for Computing Machinery. ISBN 9781450381383. doi: 10.1145/3419394.3423643. URL https://doi.org/10.1145/3419394.3423643.

Liu, S., Wei, Y., Lu, J., and Zhou, J. An improved evaluation framework for generative adversarial networks. *arXiv preprint arXiv:1803.07474*, 2018.

Lugmayr, A., Danelljan, M., Romero, A., Yu, F., Timofte, R., and Gool, L. V. Repaint: Inpainting using denoising diffusion probabilistic models. In *CVPR*, pp. 11451–11461. IEEE, 2022.

Miyato, T. and Koyama, M. cgans with projection discriminator. *arXiv preprint arXiv:1802.05637*, 2018.

Murray, N. PfaGAN: An aesthetics-conditional GAN for generating photographic fine art. In *Proceedings of the IEEE/CVF International Conference on Computer Vision Workshops*, pp. 0–0, 2019.

Odena, A., Olah, C., and Shlens, J. Conditional image synthesis with auxiliary classifier gans. In *International conference on machine learning*, pp. 2642–2651. PMLR, 2017.

Preuer, K., Renz, P., Unterthiner, T., Hochreiter, S., and Klambauer, G. Fréchet chemnet distance: a metric for generative models for molecules in drug discovery. *Journal of chemical information and modeling*, 58(9):1736–1741, 2018.

Radford, A., Kim, J. W., Hallacy, C., Ramesh, A., Goh, G., Agarwal, S., Sastry, G., Askell, A., Mishkin, P., Clark, J., Krueger, G., and Sutskever, I. Learning transferable visual models from natural language supervision, 2021.

Ramesh, A., Dhariwal, P., Nichol, A., Chu, C., and Chen, M. Hierarchical text-conditional image generation with clip latents, 2022.

Rizzato, M., Morizet, N., Maréchal, W., and Geissler, C. Stress testing electrical grids: Generative adversarial networks for load scenario generation. *Energy and AI*, 9:100177, 2022. ISSN 2666-5468. doi: https://doi.org/10.1016/j.egyai.2022.100177. URL https://www.sciencedirect.com/science/article/pii/S2666546822000295.

Rombach, R., Blattmann, A., Lorenz, D., Esser, P., and Ommer, B. High-resolution image synthesis with latent diffusion models, 2021.

Saharia, C., Chan, W., Chang, H., Lee, C. A., Ho, J., Salimans, T., Fleet, D. J., and Norouzi, M. Palette: Image-to-image diffusion models. In *NeurIPS 2021 Workshop on Deep Generative Models and Downstream Applications*, 2021.

Salimans, T. and Ho, J. Progressive distillation for fast sampling of diffusion models. In *International Conference on Learning Representations*, 2022. URL https://openreview.net/forum?id=TIdIXIpzhoI.

Sohl-Dickstein, J., Weiss, E., Maheswaranathan, N., and Ganguli, S. Deep unsupervised learning using nonequilibrium thermodynamics. In *International conference on machine learning*, pp. 2256–2265. PMLR, 2015.

Soloveitchik, M., Diskin, T., Morin, E., and Wiesel, A. Conditional frechet inception distance, 2022.

Song, Y. and Ermon, S. Generative modeling by estimating gradients of the data distribution. *Advances in Neural Information Processing Systems*, 32, 2019.

Song, Y., Sohl-Dickstein, J., Kingma, D. P., Kumar, A., Ermon, S., and Poole, B. Score-based generative modeling through stochastic differential equations. In *International Conference on Learning Representations*, 2021.

Szegedy, C., Vanhoucke, V., Ioffe, S., Shlens, J., and Wojna, Z. Rethinking the inception architecture for computer vision. *2016 IEEE Conference on Computer Vision and Pattern Recognition (CVPR)*, pp. 2818–2826, 2015.

Tashiro, Y., Song, J., Song, Y., and Ermon, S. Csdi: Conditional score-based diffusion models for probabilistic time series imputation. *Advances in Neural Information Processing Systems*, 34:24804–24816, 2021.

Thambawita, V., Isaksen, J. L., Hicks, S. A., Ghouse, J., Ahlberg, G., Linneberg, A., Grarup, N., Ellervik, C., Olesen, M. S., Hansen, T., Graff, C., Holstein-Rathlou, N.-H., Strümke, I., Hammer, H. L., Maleckar, M. M., Halvorsen, P., Riegler, M. A., and Kanters, J. K. Deepfake electrocardiograms using generative adversarial networks are the beginning of the end for privacy issues in medicine. *Scientific Reports*, 11(1):21896, 2021. doi: 10.1038/s41598-021-01295-2. URL https://doi.org/10.1038/s41598-021-01295-2.

Trindade, A. Electricity Load Diagrams. UCI Machine Learning Repository, 2015. DOI: https://doi.org/10.24432/C58C86.

Unterthiner, T., van Steenkiste, S., Kurach, K., Marinier, R., Michalski, M., and Gelly, S. Towards accurate generative models of video: A new metric & challenges. *arXiv preprint arXiv:1812.01717*, 2018.

Wagner, P., Strodthoff, N., Bousseljot, R.-D., Kreiseler, D., Lunze, F. I., Samek, W., and Schaeffter, T. Ptb-xl, a large publicly available electrocardiography dataset. *Scientific data*, 7(1):154, 2020.

Wu*, Y., Chen*, K., Zhang*, T., Hui*, Y., Berg-Kirkpatrick, T., and Dubnov, S. Large-scale contrastive language-audio pretraining with feature fusion and keyword-to-caption augmentation. In *IEEE International Conference on Acoustics, Speech and Signal Processing, ICASSP*, 2023.

Yoon, J., Jarrett, D., and van der Schaar, M. Time-series generative adversarial networks. In Wallach, H., Larochelle, H., Beygelzimer, A., d'Alché-Buc, F., Fox, E., and Garnett, R. (eds.), *Advances in Neural Information Processing Systems*, volume 32. Curran Associates, Inc., 2019. URL https://proceedings.neurips.cc/paper_files/paper/2019/file/c9efe5f26cd17ba6216bbe2a7d26d490-Paper.pdf.

Yoon, J., Drumright, L., and Schaar, M. Anonymization through data synthesis using generative adversarial networks (ads-gan). *IEEE Journal of Biomedical and Health Informatics*, PP:1–1, 03 2020. doi: 10.1109/JBHI.2020.2980262.

Yuan, X., Lin, Z. L., Kuen, J., Zhang, J., Wang, Y., Maire, M., Kale, A., and Faieta, B. Multimodal contrastive training for visual representation learning. *2021 IEEE/CVF Conference on Computer Vision and Pattern Recognition (CVPR)*, pp. 6991–7000, 2021. URL https://api.semanticscholar.org/CorpusID:233407906.

Zhang, Y., Jiang, H., Miura, Y., Manning, C. D., and Langlotz, C. P. Contrastive learning of medical visual representations from paired images and text. In Lipton, Z., Ranganath, R., Sendak, M., Sjoding, M., and Yeung, S. (eds.), *Proceedings of the 7th Machine Learning for Healthcare Conference*, volume 182 of *Proceedings of Machine Learning Research*, pp. 2–25. PMLR, 05–06 Aug 2022. URL https://proceedings.mlr.press/v182/zhang22a.html.

Zhou, H., Zhang, S., Peng, J., Zhang, S., Li, J., Xiong, H., and Zhang, W. Informer: Beyond efficient transformer for long sequence time-series forecasting. In *Proceedings of the AAAI conference on artificial intelligence*, volume 35, pp. 11106–11115, 2021.

# Appendix

## A. Diffusion Process

DMs are trained to denoise a noisy sample, referred to as the backward process $p_\theta$, generated by a Markovian forward process $q$. The forward process is predetermined by specifying a noise schedule $\{\beta_1, \ldots, \beta_T\}$. The following equations parameterize the forward process:

$$q(x_1, \ldots, x_T \mid x_0) = \prod_{t=1}^{T} q(x_t \mid x_{t-1}), \tag{7}$$

$$q(x_t \mid x_{t-1}) = \mathcal{N}(\sqrt{1 - \beta_t} x_{t-1}, \beta_t \mathbf{I}). \tag{8}$$

where $x_0 \sim \mathcal{X}$ and $T$ is the number of diffusion steps. The noise schedule $\{\beta_1, \ldots, \beta_T\}$ and $T$ are chosen such that the distribution of $x_T$ is zero-mean, unit-variance normal distribution, i.e., $q(x_T) \simeq \mathcal{N}(\mathbf{0}, \mathbf{I})$. This allows us to start the backward process from $x_T \sim \mathcal{N}(\mathbf{0}, \mathbf{I})$ and iteratively denoise for $T$ steps to obtain a sample from $\mathcal{X}$. The reverse process is parameterized as follows:

$$p_\theta(x_0, \ldots, x_{T-1} \mid x_T) = p(x_T) \prod_{t=1}^{T} p_\theta(x_{t-1} \mid x_t). \tag{9}$$

Here, $p(x_T) = \mathcal{N}(\mathbf{0}, \mathbf{I})$. Essentially, the reverse process is learnable, and $p_\theta(x_{t-1} \mid x_t)$ approximates $q(x_{t-1} \mid x_t, x_0)$. Ho et al. (2020) show that through simple reparametrization tricks, we can convert the learning objective from approximating $q(x_{t-1} \mid x_t, x_0)$ to estimating the amount of noise added to go from $x_{t-1}$ to $x_t$. Thus, the diffusion objective is stated as minimizing the following loss function:

$$\mathcal{L}_{\text{DM}} = \mathbb{E}_{x \sim \mathcal{X}, \epsilon \sim \mathcal{N}(\mathbf{0}, \mathbf{I}), t \sim \mathcal{U}(1, T)} [\|\epsilon - \theta_{\text{denoiser}}(x_t, t)\|_2^2]. \tag{10}$$

where $t \sim \mathcal{U}(1, T)$ indicates that $t$ is sampled from a uniform distribution between 1 and $T$, $\epsilon$ is the noise added to $x_{t-1}$ to obtain $x_t$, and $\theta_{\text{denoiser}}$ is parameterized by a neural network that takes the noisy sample $x_t$ and the diffusion step $t$ as input to estimate $\epsilon$. This is equivalent to score-matching techniques (Song & Ermon, 2019; Song et al., 2021).

## B. Dataset Description

In this section, we describe in detail the various datasets used in our experiments, the training, validation, and testing dataset splits, and the normalization procedure that was opted.

### B.1. Electricity Dataset

The electricity dataset consists of power consumption recorded for 370 users over a period of 4 years from 2011 to 2015. We frame the following task with respect to this dataset - "Generate the electricity demand pattern for the user 257, for the 3rd of August 2011," which is a univariate time series. We consider the following features as the metadata - 370 users, 4 years, 12 months, and 31 dates (check Table 3). The power consumption is recorded every 15 minutes, so the time series is 96 timesteps long. The total number of samples without any preprocessing is 540200. We remove samples with values as 0 for the entire time series, and the resulting total number of samples is 434781. We establish a data split comprising training, validation, and test sets distributed in an 80-10-10 ratio. To obtain the split, we randomly pick 80% of the 434781 samples and assign them as the training set. The same is repeated for the validation and the test sets. We avoid using the traditional splits proposed in (Du et al., 2023) as their split creates certain year metadata features that never existed in the training set. For example, no month from 2011 exists in the training set.

### B.2. Traffic Dataset

For traffic volume synthesis, we use the metro interstate traffic volume dataset. The dataset has hourly traffic volume recorded from 2012 to 2018, along with metadata annotations like holidays, textual weather descriptions, weather forecasts,

| DATASET | HORIZON | # CHANNELS | CATEGORICAL FEATURES | CONTINUOUS FEATURES |
|---------|---------|-----------|---------------------|---------------------|
| AIR QUALITY | 96 | 6 | 12 STATIONS, 5 YEARS, 12 MONTHS, 31 DATES, 24 HOURS, 17 WIND DIRECTIONS | TEMPERATURE, PRESSURE, DEW POINT TEMPERATURE, RAIN LEVELS, WIND SPEED |
| TRAFFIC | 96 | 1 | 12 HOLIDAYS, 7 YEARS, 12 MONTHS, 31 DATES, 24 HOURS, 11 BROAD WEATHER DESCRIPTIONS, 38 FINE WEATHER DESCRIPTIONS | TEMPERATURE, RAIN LEVELS, SNOWFALL LEVELS, CLOUD CONDITIONS |
| ELECTRICITY | 96 | 1 | 370 USERS, 4 YEARS, 12 MONTHS, 31 DATES | NA |
| ECG | 1000 | 12 | 71 HEART DISEASE STATEMENTS | NA |

*Table 3.* **Dataset overview for experiments with TIME WEAVER.** This table outlines the key characteristics of the datasets employed in our experiments. These datasets, encompassing Air Quality, Traffic, Electricity, and ECG, have been carefully selected to demonstrate TIME WEAVER's versatility across different time horizons, number of channels, and a wide range of metadata types.

etc. (check Table 3). Here, we want to answer questions like - "Synthesize a traffic volume pattern for New Year's Day, given the weather forecast", which is a univariate time series. The dataset CSV file has a total of 48204 rows containing the traffic volume. We synthesize the traffic volume for a 96-hour window. So, to create a dataset from the CSV file, we slide a window of length 96 with a stride of 24. This gives a total of 2001 time series samples, which we randomly divide into train, validation, and test split with an 80-10-10 ratio.

### B.3. Air Quality Dataset

This data set contains hourly air pollutants data from 12 air-quality monitoring stations in Beijing. The meteorological data in each air-quality site are paired with the weather data from the nearest weather station (check Table 3 for more details regarding the metadata conditions). Here, the task is to synthesize a multivariate time series (6 channels) given the weather forecast metadata. The dataset has missing values, which we replace with the mean for both continuous metadata and the time series. For categorical metadata, the only missing feature is the wind direction, which we fill using an "unknown" label. The data set is split into train, validation, and test splits based on months. The recordings are available from 2013 to 2017, and we have a total of 576 months, of which we randomly pick 460 as train, 58 as validation, and 58 as test. For each month, we slide a window of length 96 with a stride of 24, and this provides a total of 12166 train time series samples, 1537 validation time series samples, and 1525 test time series samples.

### B.4. ECG Dataset

The PTB-XL ECG dataset is a 12-channel, 1000 time steps long, time series dataset with 17651 train, 2203 validation, and 2167 test samples. The dataset has annotated heart disease statements for each ECG time series. Here, the goal is to attempt to generate ECG time series samples for a specific heart disease statement, which is our metadata. In this work, we use 8 channels instead of 12, as shown in (Alcaraz & Strodthoff, 2023).

## C. Metric model architecture description

To compute our proposed J-FTSD metric, we relied on the Informer encoder architecture proposed in (Zhou et al., 2021). Specifically, we used two encoders, one for the time series and one for the metadata features, represented as $\phi_{\text{time}}$ and $\phi_{\text{meta}}$, respectively. We made the following modifications to the Informer encoder architecture:

- The raw time series is first processed using 1D convolution layers, and we added positional encoding to the processed time series before providing as input to the self-attention layers in $\phi_{\text{time}}$. We used the same positional encoding as in the Informer (Zhou et al., 2021).
- The raw metadata is processed in the same way as we processed metadata for the diffusion process, which is highlighted in Sec. 4. We individually processed or tokenized the categorical and continuous metadata using linear layers and 1D convolution layers to obtain $z$. We added positional encoding to $z$ before providing $z$ as input to the self-attention layers in $\phi_{\text{meta}}$.
- We used 1D convolution layers at the end of every self-attention layer without any striding. We used striding after every 3 self-attention layers, i.e., the 1D convolution layers with stride of 2 is applied after the $3^{rd}$, $6^{th}$, ..., self-attention layers.
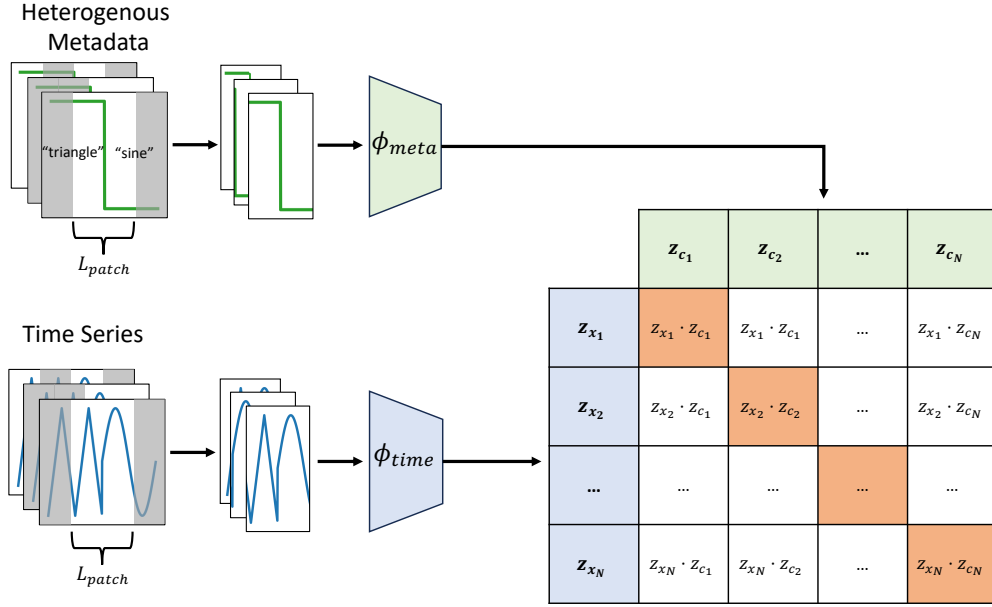
*Figure 6.* **Contrastive Training of J-FTSD Feature Extractors Inspired by CLIP (Radford et al., 2021):** This figure depicts the contrastive learning-based training approach for the J-FTSD feature extractors $\phi_{\text{time}}$ and $\phi_{\text{meta}}$, akin to the methodology used in CLIP. Here, we consider a time series where the first half is a triangle wave and the second half is a sine wave. The categorical metadata corresponds to this pattern, with the first half labeled as 1 ("triangle") and the second half as 0 ("sine"). Patches of length $L_{\text{patch}}$ are extracted from time series and metadata and processed through their respective feature extractors. The embeddings, $z^c$ from metadata and $z^x$ from time series, are compared using their dot products to identify correct pairings, highlighted along the matrix diagonal (in orange). The feature extractors are trained through contrastive learning, employing cross-entropy loss to enhance the accuracy of matching time series data with its relevant metadata, effectively capturing the nuanced relationship between the two.

- At the end of the self-attention layers of both $\phi_{\text{time}}$ and $\phi_{\text{meta}}$, we flattened the outputs and projected the outputs to a lower-dimensional space using linear layers. We used the Gaussian Error Linear Unit (GELU) activation, the same as in the Informer architecture.

Now, we describe the choice of $L_{\text{patch}}$ for each dataset. As explained in Sec. 5, we chose $L_{\text{patch}}$ based on the minimum horizon required for a patch to contain metadata-specific features. Now, we describe the values of $L_{\text{patch}}$ and the embedding size, which is the dimension of the output of the feature extractors:

| DATASET | $L_{\text{patch}}$ | EMBEDDING SIZE |
|---|---|---|
| AIR QUALITY | 64 | 128 |
| ECG | 256 | 256 |
| ELECTRICITY | 64 | 48 |
| TRAFFIC | 64 | 48 |

*Table 4.* **Patch and Embedding sizes of all datasets.**

Specifically, we chose the embedding size such that given a time series sample $x \in \mathbb{R}^{L \times F}$, where $L$ is the horizon and $F$ is the number of channels in the time series, the embedding size should be smaller than $F \times L_{\text{patch}}$. This is to ensure that we are reducing the dimensionality of the time series patch.

Now, we list the hyperparameter choices, such as the number of patches from a single time series sample $N_{\text{patch}}$, learning rate, etc, and the design choices in terms of the number of self-attention layers, number of transformer heads, etc.

| DESIGN PARAMETER | VALUE |
|---|---|
| EMBEDDING SIZE (`dmodel`) | 128 |
| ATTENTION HEADS (`nheads`) | 8 |
| SELF-ATTENTION LAYERS | 8 |
| DROPOUT | 0.05 |
| ACTIVATION | GELU |
| $N_{\text{patch}}$ | 2 |
| LEARNING RATE | $10^{-4}$ |

*Table 5.* **Hyperparamters for Feature Extractors.**

# D. TIME WEAVER architecture design

As mentioned in Sec. 4, TIME WEAVER has two denoiser backbones - CSDI (Tashiro et al., 2021) and SSSD (Alcaraz & Strodthoff, 2023). In this section, we describe the architecture changes we introduced to the CSDI and the SSSD backbones to extend their capabilities to metadata-conditioned time series generation.

## D.1. TIME WEAVER-CSDI



*Figure 7.* **TIME WEAVER-CSDI architecture:** This figure shows our changes to the original conditional CSDI model (Tashiro et al., 2021). We use this model as a $\theta_{\text{denoiser}}$ model in our architecture, with metadata preprocessing fixed as in Fig. 3. Changes in the original architecture are colored red.

Consider a batch of time series samples of size $(N_{\text{batch}}, F, L)$, where $N_{\text{batch}}$ represents the number of samples per batch, $F$ represents the number of channels in the time series, and $L$ represents the horizon. The paired metadata is represented as $c_{\text{cat}} \oplus c_{\text{cont}}$, where the shape of $c_{\text{cat}}$ is $(N_{\text{batch}}, L, K_{\text{cat}})$ and the shape of $c_{\text{cont}}$ is $(N_{\text{batch}}, L, K_{\text{cont}})$.

- *Input time series projection:* We first transformed the input time series batch to $(N_{\text{batch}} \times F, 1, L)$ and applied 1D convolution layers with $d_{\text{meta}}$ filters to obtain a projection of shape $(N_{\text{batch}} \times F, d_{\text{meta}}, L)$. We then reshaped the projection from $(N_{\text{batch}} \times F, d_{\text{meta}}, L)$ to $(N_{\text{batch}}, d_{\text{meta}}, F, L)$.
- *Metadata projection:* Simultaneously, we converted each categorical metadata feature in $c_{\text{cat}}$ into one-hot encoding and further process using $\theta_{\text{token}}^{\text{cat}}$. We processed the continuous metadata, $c_{\text{cont}}$, using $\theta_{\text{token}}^{\text{cont}}$. Both $c_{\text{cat}}$ and $c_{\text{cont}}$ are

| Design Parameter | Value |
|---|---|
| Position embedding | 128 |
| Feature or Channel embedding | 16 |
| Diffusion step embedding | 256 |
| Embedding size ($d_{\text{meta}}$) | 256 |
| Attention heads (`nheads`) | 16 |
| Metadata encoder ($\theta_{\text{condn}}$) embedding size | 256 |
| Metadata encoder ($\theta_{\text{condn}}$) attention heads | 8 |
| Metadata encoder ($\theta_{\text{condn}}$) self-attention layers | 2 |
| Learning rate | $10^{-4}$ |

*Table 6.* **Hyperparameters for TIME WEAVER-CSDI Architecture.**

projected to latent representations of shape $(N_{\text{batch}}, L, d_{\text{cat}})$ and $(N_{\text{batch}}, L, d_{\text{cont}})$. We concatenated these latent representations along the final axis and processed them using self-attention layers, $\theta_{\text{condn}}$. At the end of this preprocessing, the categorical and continuous metadata were projected to a latent representation of shape $(N_{\text{batch}}, L, d_{\text{meta}})$. We then reshaped the projected metadata to $(N_{\text{batch}}, d_{\text{meta}}, F, L)$.

- *Diffusion step representation:* The CSDI architecture represents the diffusion step using a 128-dimensional representation, which is projected to $d_{\text{meta}}$. We later reshaped the diffusion step representation to $(N_{\text{batch}}, d_{\text{meta}}, F, L)$.
- We added the input time series projection, metadata projection, and diffusion step representation and passed it through temporal and feature transformer layers in the first residual layer.
- We provided the projected metadata as input to all the residual layers in the same manner.

For the diffusion process, our experiments with TIME WEAVER-CSDI use 200 diffusion steps with the noise variance schedule values of $\beta_1 = 0.0001$ and $\beta_T = 0.1$

Now, we explain the architectural details and the corresponding hyperparameters. The number of residual layers used varies for each dataset. For the Air Quality dataset, we used 10 residual layers. Similarly, for the Traffic, Electricity, and ECG datasets, we used 8,6, and 12, respectively.

### D.2. TIME WEAVER-SSSD

The TIME WEAVER-SSSD model is based on the structured state-space diffusion (SSSD) model (Alcaraz & Strodthoff, 2022) that was originally designed for the imputation task. The SSSD model is built on DiffWave (Kong et al., 2021) architecture. Unlike the DiffWave model, SSSD utilizes structured state-space models (SSM) (Gu et al., 2022), which connects input sequence $u(t)$ to output sequence $y(t)$ via hidden state $x(t)$. This relation can be explicitly given as:

$$x'(t) = Ax(t) + Bu(t) \quad \text{and} \quad y(t) = Cx(t) + Du(t).$$

Here, $A, B, C, D$ are transition matrices that are learned. Gu et al. (2022) propose stacking several SSM blocks together to create a Structured State Space sequence model (S4). Then, these SSM blocks are connected with normalization layers and point-wise FC layers in a way that resembles the transformer architecture. This architectural change is done to capture long-term dependencies in time series data. Alcaraz & Strodthoff (2023) adjusts this architecture to take label input, a binary vector of length 71. As shown in Fig. 8, we replaced this label input with the metadata embeddings obtained with our metadata preprocessing block to incorporate more various metadata modalities. We saw that this generates the best quality examples, and the remaining architecture is kept the same.

For the diffusion process, our experiments with TIME WEAVER-SSSD used 200 diffusion steps with the noise variance schedule values of $\beta_1 = 0.0001$ and $\beta_T = 0.02$

Now, we provide the list of design choices and hyperparameter choices used in the TIME WEAVER-SSSD model.
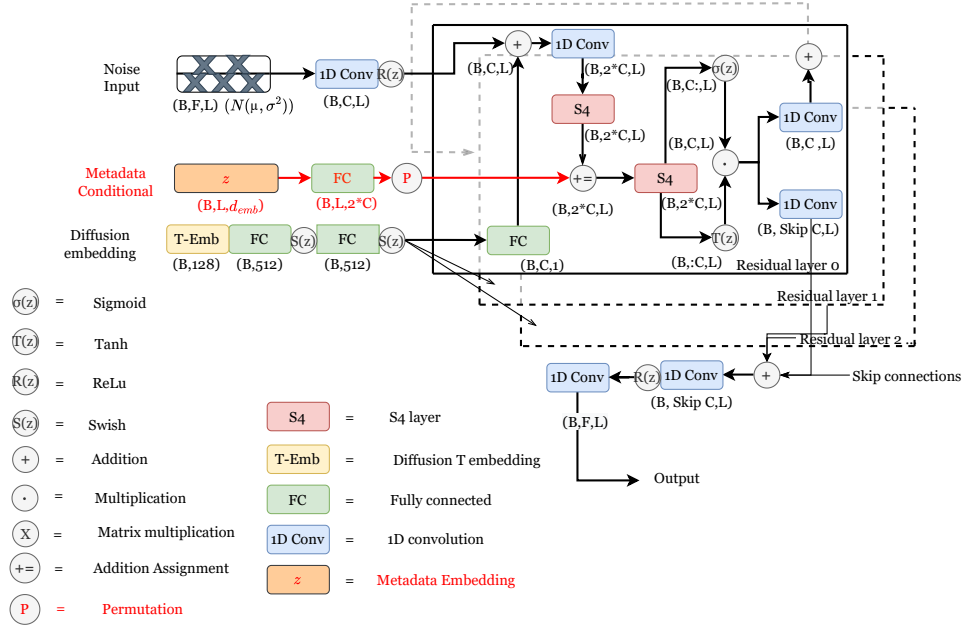
*Figure 8.* **TIME WEAVER-SSSD architecture:** This figure shows our changes to the original conditional SSSD model (Alcaraz & Strodthoff, 2023). We use this model as a $\theta_{\text{denoiser}}$ model in our architecture, with metadata preprocessing being fixed as in Fig. 3. Changes to the original architecture are highlighted in red.

| DESIGN PARAMETER | VALUE |
|---|---|
| RESIDUAL LAYER CHANNELS | 256 |
| SKIP CHANNELS | 16 |
| DIFFUSION STEP EMBEDDING INPUT CHANNELS | 128 |
| DIFFUSION STEP EMBEDDING MID CHANNELS | 512 |
| DIFFUSION STEP EMBEDDING OUTPUT CHANNELS | 512 |
| S4 LAYER STATE DIMENSION | 64 |
| S4 LAYER DROPOUT | 0.0 |
| IS S4 LAYER BIDIRECTIONAL | TRUE |
| USE LAYER NORMALIZATION | TRUE |
| METADATA ENCODER ($\theta_{\text{condn}}$) EMBEDDING SIZE | 256 |
| METADATA ENCODER ($\theta_{\text{condn}}$) ATTENTION HEADS | 8 |
| METADATA ENCODER ($\theta_{\text{condn}}$) SELF-ATTENTION LAYERS | 2 |
| LEARNING RATE | $10^{-4}$ |

*Table 7.* **Hyperparameters for TIME WEAVER-SSSD Architecture.**

## E. GAN baselines

### E.1. Main GAN baselines

For our main GAN baselines, we used Pulse2PulseGAN (Thambawita et al., 2021) and WaveGAN (Donahue et al., 2019). Since these approaches are not fundamentally conditional, we added additional layers to enable conditional generation.

- For the Electricity and the ECG datasets, we used the implementation provided by (Thambawita et al., 2021) and (Alcaraz & Strodthoff, 2023). Since these datasets only have categorical metadata, we represented each categorical label by a fixed embedding. This fixed embedding was added to the output of each layer in the generator after the

batch normalization layers. Similarly, we added the fixed embedding to the output of each layer in the discriminator. To learn the conditional distribution, along with predicting whether a sample is real or fake, we also predicted the logit of each categorical metadata, similar to (Odena et al., 2017). In our experiments, we noticed that predicting the metadata category for the fake sample rarely helps and provides poor-quality samples. Hence, we only predicted the category for the real samples.
- For the Air Quality and Traffic datasets, we appended the inputs to the generator and discriminator with the metadata conditions.

For all the datasets except the Air Quality dataset, we used min-max normalization to transform the time series samples to lie between -1 and 1. For the Air Quality dataset, we used the standard zero mean, unit variance normalization.

### E.1.1. WAVEGAN IMPLEMENTATION DETAILS

We trained the WaveGAN model for all the datasets for 1500 epochs with a learning rate of $10^{-4}$ and stored the checkpoints after every 100 epochs. We sampled noise, a $48$ dimensional vector for the Electricity, Air Quality, and Traffic datasets, and a 100 dimensional vector for ECG. We relied on the `pytorch` implementation (Link to the repo) of WaveGAN and (Alcaraz & Strodthoff, 2023) for our experiments. We adjusted the number of parameters in the generator and discriminator to roughly match the TIME WEAVER models.

- For the Air Quality dataset, the total number of trainable parameters in the GAN model is 15.2 million and the generator has 8.51 million trainable parameters.
- For the Traffic dataset, the total number of trainable parameters in the GAN model is 13.7 million and the generator has 7.017 million trainable parameters.
- For the Electricity dataset, the total number of trainable parameters in the GAN model is 13.3 million and the generator had 7.17 million parameters.
- For the ECG dataset, the total number of trainable parameters in the GAN model is 40.9 million, and the generator has 21.36 million parameters.

### E.1.2. PULSE2PULSEGAN IMPLEMENTATION DETAILS

We trained the Pulse2PulseGAN model in the same manner as the WaveGAN for all the datasets. We trained the Pulse2PulseGAN model for 1500 epochs with a learning rate of $10^{-4}$ and stored the checkpoints after every 100 epochs. Here, the noise input to the generator had the same dimensions as the time series sample that we wanted to generate. We adjusted the number of parameters in the generator and discriminator to roughly match the TIME WEAVERmodels.

- For the Air Quality dataset and the Traffic, the total number of trainable parameters in the GAN model is 14.1 million and the generator has 7.45 million trainable parameters.
- For the Electricity dataset, the total number of trainable parameters in the GAN model is 16.9 million and the generator has 8.4 million parameters.
- For the ECG dataset, the total number of trainable parameters in the GAN model is 43 million, and the generator has 23.47 million parameters.

### E.2. Additional GAN baselines

In addition to WaveGAN (Donahue et al., 2019) and Pulse2Pulse (Thambawita et al., 2021) models, we have implemented TTS-GAN (Li et al., 2022) and well-established TimeGAN (Yoon et al., 2019) method. Unfortunately, we were unable to train these models to generate effectively. These models were likely challenged by higher input lengths than their original implementation, where TimeGAN and TTS-GAN consider time steps up to 24 and 188, respectively, while we consider time steps of up to 1000. A similar problem was also faced in literature (Alcaraz & Strodthoff, 2023). We include our training examples after 10000 epochs for the traffic dataset in Figure 9.
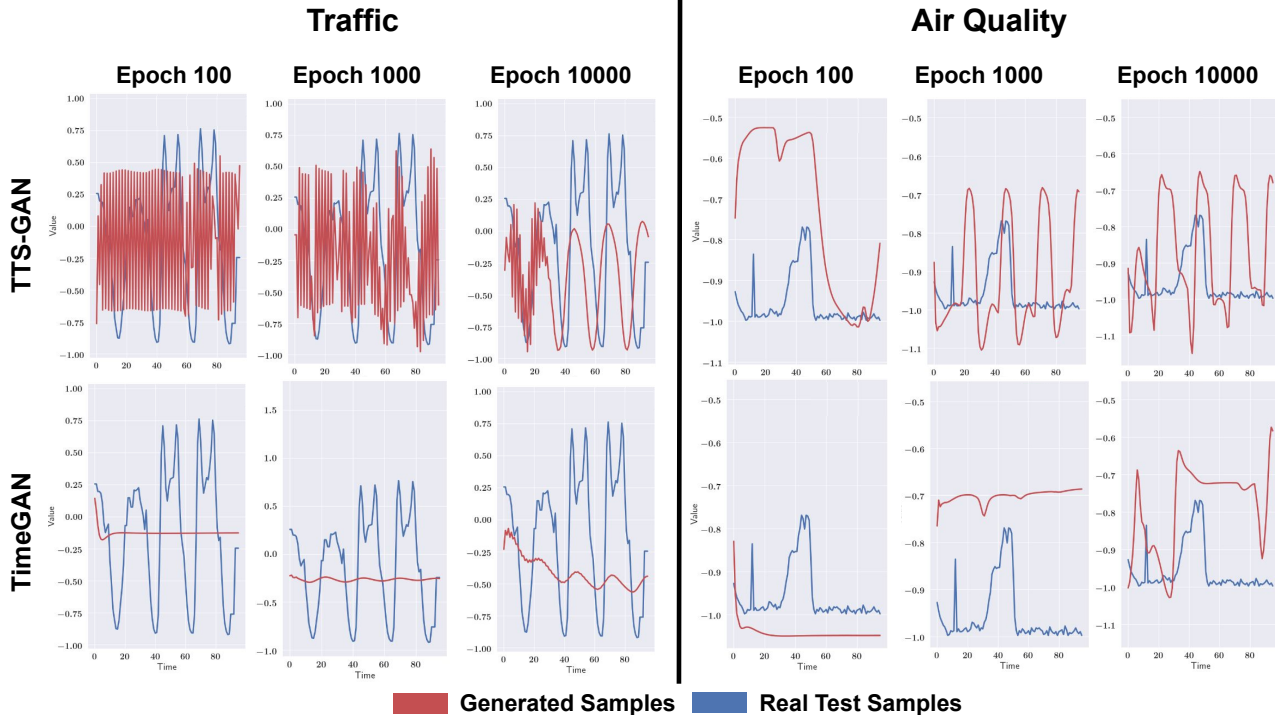
*Figure 9.* **TimeGAN and TTS-GAN failed to generate realistic samples after 10000 epochs** This figure shows the samples generated for the test examples after 100, 1000, and 10000 training epochs, where *row 1* and *row 2* correspond to TTS-GAN and TimeGAN respectively. We can clearly see that both models fail to generate high-quality realistic samples.

## F. Evaluation Metrics

In this section, we briefly describe the details regarding the evaluation metrics, i.e., TSTR (train on synthetic test on real) and J-FTSD.

### F.1. J-FTSD details

For the Electricity, Air Quality, and Traffic datasets, the horizon is 96, i.e., $L = 96$. So, we took time series and metadata patches of length $L_{\text{patch}} = 64$ from time step 1, i.e., 1 to 64, 2 to 65, ..., and obtained the time series and the metadata embeddings using $\phi_{\text{time}}$ and $\phi_{\text{meta}}$ respectively. We computed the J-FTSD from these embeddings using Eq. (6). For the ECG dataset, since the horizon is 1000, and the patch length is 256, we sampled patches of length 256 after every 10 time steps, i.e., 1 to 256, 10 to 266, etc.

One of the key points to be noted is that the feature extractors, $\phi_{\text{time}}$, and $\phi_{\text{meta}}$, are trained on the entire data distribution. This was done to ensure that the inefficiency of the feature extractors to extract accurate and metadata-specific features should not affect the evaluation process, which can occur when the feature extractors are trained on a training split alone. Therefore, we trained the feature extractors on the entire dataset to evaluate generative models.

### F.2. Train on Synthetic Test on Real details (TSTR)

For TSTR, we use a standard ResNet 1D (He et al., 2016) architecture. We performed the following classification tasks:

* Classification over months in the Electricity dataset. There are 12 classes in total and we trained the classifier with cross-entropy loss for 500 epochs with a learning rate of $10^{-4}$.
* Classification over heart disease statements in the ECG dataset. There are 71 classes and for a given time series sample, more than one class could be active. So, we trained a classifier with binary cross-entropy loss for 500 epochs with a learning rate of $10^{-4}$.

- Classification over the coarse weather description in the Traffic dataset. 11 coarse weather descriptions are available as annotations for each time step in the traffic dataset. To this end, we treated the classification task here as a multi-class, multi-label classification problem. So, we trained a classifier with binary cross-entropy loss for 200 epochs with a learning rate of $10^{-4}$.
- Classification over 12 weather stations for the Air Quality dataset. We used the cross-entropy loss for 200 epochs with a learning rate of $10^{-4}$.

Here, we note that with the trained diffusion model, we generated the synthetic train, validation, and test datasets. The classifier is trained on the synthetic train dataset, and the checkpoints are stored with the synthetic validation dataset. We finally evaluated the model on the real test dataset.

## G. Additional Qualitative Results

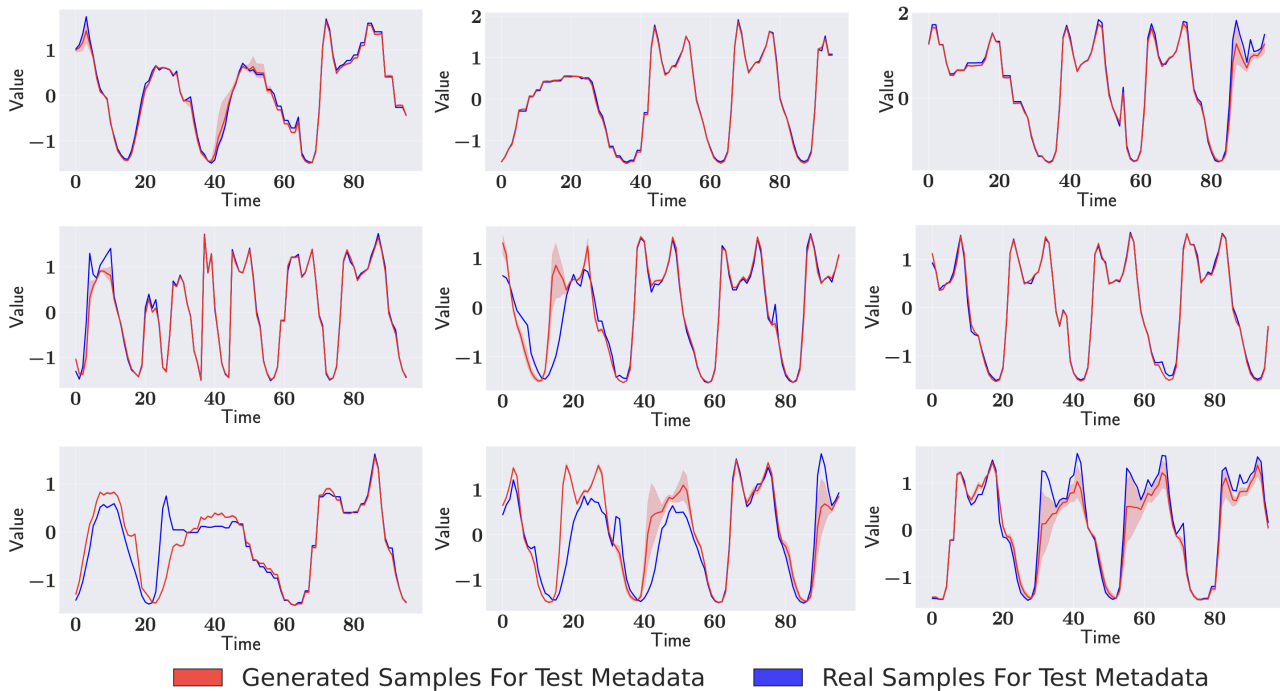In this section, we provide additional qualitative results generated using TIME WEAVER.



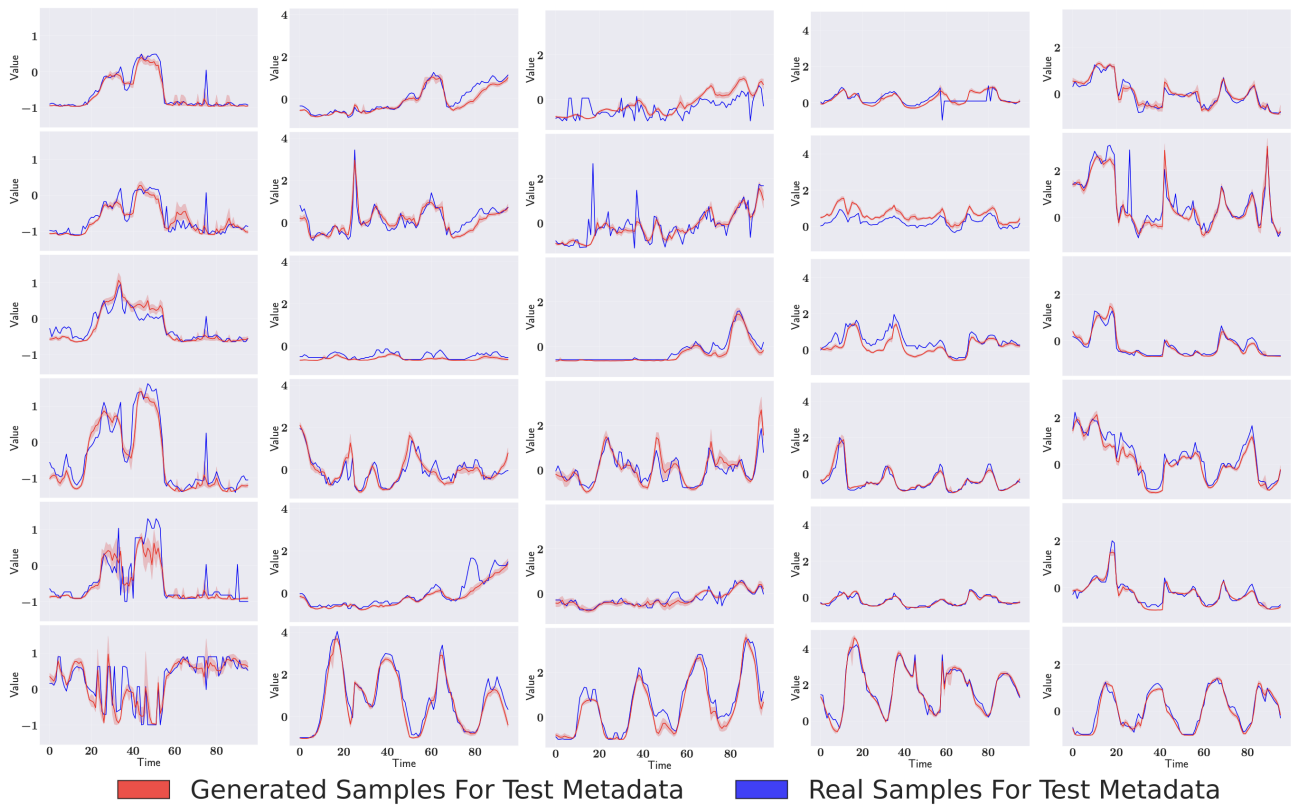Figure 10. TIME WEAVER-CSDI Qualitative Results for Traffic Dataset

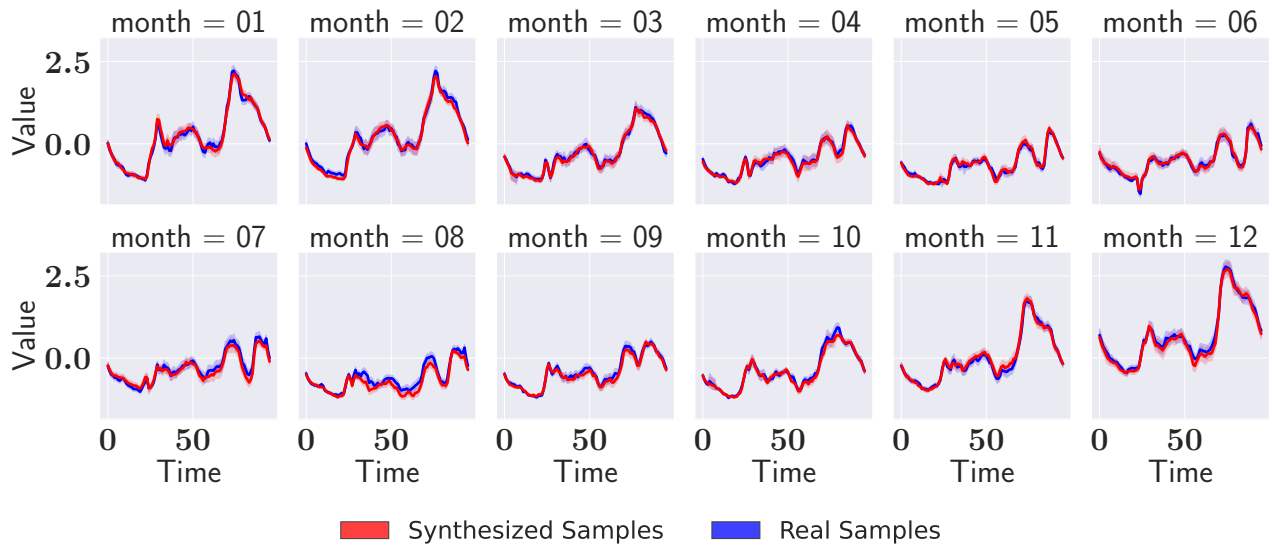*Figure 11.* TIME WEAVER-CSDI Qualitative Results for the Air Quality Dataset



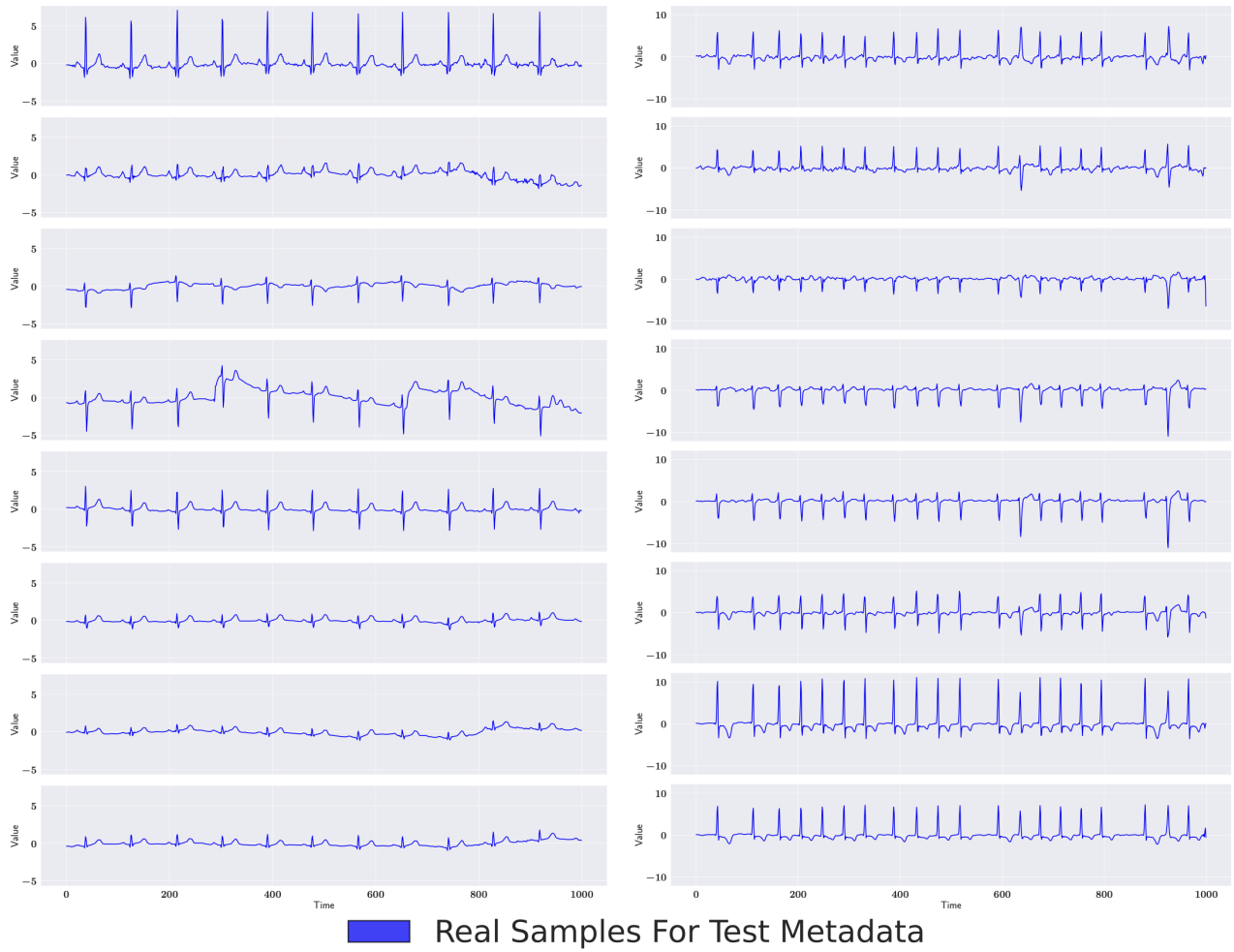*Figure 14.* **Generated time series samples from the Electricity Dataset**

*Figure 12.* **Real time series samples from the ECG Dataset**

*Figure 13.* **Generated time series samples from the ECG Dataset**